Clinical Cancer Research

Distinct Interactions Between c-Src and c-Met in Mediating Resistance to c-Src Inhibition in Head and Neck Cancer

Banibrata Sen[1], Shaohua Peng[1], Babita Saigal[1], Michelle D. Williams[1,2], and Faye M. Johnson[1,3]

Abstract

Purpose: c-Src inhibition in cancer cells leads to an abrogation of invasion but a variable effect on apoptosis. The pathways downstream of c-Src promoting survival are not well characterized. Because cancer therapy that both decreases invasion and induces significant apoptosis would be ideal, we sought to characterize the mechanisms of resistance to c-Src inhibition.

Experimental Design: c-Src was inhibited in a panel of oral cancer cell lines and subsequent survival and signaling measured. The interactions between c-Src and c-Met were evaluated using immunoprecitation and an *in vitro* kinase assay. Cytotoxicity was measured and the Chou–Talalay combination index calculated. An orthotopic model of oral cancer was used to assess the effects of c-Met and c-Src inhibitors.

Results: Inhibition of c-Src resulted in c-Met inhibition in sensitive cells lines, but not in resistant cell lines. Isolated c-Met was a c-Src substrate in both sensitive and resistant cells, but there was no interaction of c-Src and c-Met in intact resistant cells. To examine the biological consequences of this mechanism, we demonstrated synergistic cytotoxicity, enhanced apoptosis, and decreased tumor size with the combination of c-Src and c-Met inhibitors.

Conclusions: Sustained c-Met activation can mediate resistance to c-Src inhibition. These data suggest that the differences between c-Met and c-Src signaling in sensitive and resistant cells are due to distinct factors promoting or inhibiting interactions, respectively, rather than to intrinsic structural changes in c-Src or c-Met. The synergistic cytotoxic effects of c-Src and c-Met inhibition may be important for the treatment of head and neck cancers. *Clin Cancer Res; 17(3); 514–24. ©2010 AACR.*

Introduction

All epithelial tumors pose formidable challenges in clinical practice, but the anatomy of tumors in the head and neck region makes them particularly difficult to treat. Approximately 45,000 new cases of head and neck cancer are diagnosed in the United States each year, and the estimated worldwide incidence is 500,000 (1). The incidence and survival statistics are only half of the story, however; cancer- and treatment-induced distortions of anatomy and physiology have a profound impact on important functions such as eating, speaking, and hearing, and distortions in facial appearance contribute to social isolation in survivors. Although novel approaches have improved locoregional control in patients with advanced head and neck squamous cell carcinoma (HNSCC), locoregional and distant recurrence remains common and is almost always fatal. Thus, there is a great need to improve systemic therapy for patients with these tumors to increase cure rates and reduce morbidity.

The most successful targeted molecular therapeutic approach is inhibition of oncogene targets, particularly tyrosine kinases. One potential oncogene target in HNSCC is the c-Src family of nonreceptor tyrosine kinases (SFKs) (2, 3). Aberrant activation of c-Src has been demonstrated in numerous epithelial tumors, including HNSCC. c-Src regulates multiple signaling cascades that control diverse biological processes, and its inhibition in cancer cells can lead to reduced anchorage-independent growth, proliferation, survival, invasion, migration, metastasis, and tumor vascularity (2). In epithelial cancers, however, several researchers have observed that, while c-Src inhibition decreases migration and invasion, it has little effect on proliferation or apoptosis (4–6). In 10 of 12 colon cancer cell lines, complete inhibition of c-Src activity did not affect cell proliferation, although it did inhibit adhesion and migration (7). Similarly, c-Src inhibition in pancreatic cancer cells had no effect on cell cycle progression but completely inhibited migration and angiogenesis (8). We demonstrated that c-Src inhibition resulted in a universal and profound reduction of invasion and migration of all

Authors' Affiliation: [1]Departments of Thoracic/Head and Neck Medical Oncology and [2]Pathology, The University of Texas MD Anderson Cancer Center, Houston; [3]The University of Texas Graduate School of Biomedical Sciences at Houston, Houston, Texas

Note: Supplementary data for this article are available at Clinical Cancer Research Online (http://clincancerres.aacrjournals.org/).

Corresponding Author: Faye M. Johnson, Department of Thoracic/Head and Neck Medical Oncology, Unit 432, The University of Texas MD Anderson Cancer Center, 1515 Holcombe Blvd., Houston, TX 77030-4009. Phone: 713-792-6363; Fax: 713-792-1220; E-mail: fmjohns@mdanderson.org.

doi: 10.1158/1078-0432.CCR-10-1617

Translational Relevance

Although invasion is important in the pathophysiology of many cancers, local invasion is critical in head and neck cancers as a determinant of both morbidity and mortality, as it is associated with poorer locoregional control and decreased survival. Cancer therapy that both induces significant apoptosis and decreases invasion would be ideal for head and neck cancer. Because c-Src inhibition leads to profoundly diminished invasion with only moderate effects on survival and proliferation, we sought to identify pathways leading to cytotoxicity downstream of c-Src. Here we demonstrate that sustained c-Met activation mediates cell survival following c-Src inhibition. We investigated the biological importance of this interaction and discovered that c-Src and c-Met inhibition were synergistic. Given that both c-Src and c-Met inhibitors are in clinical use, our studies are immediately relevant for human cancer treatment.

HNSCC cell lines, but produced cytotoxicity in only 4 of 9 HNSCC cell lines (9, 10). Clearly, c-Src can mediate distinct biological processes independently. This may be accomplished by differential effects of c-Src on its multiple downstream substrates.

Although the molecular mechanisms that mediate c-Src's effects on migration have been well described (11), those that mediate proliferation and survival are less well defined. c-Src can mediate its effects on proliferation and survival via interactions with growth factor receptors as well as the ERK1/2, JAK/STAT, and phosphoinositide 3-kinase (PI3K) pathways. c-Src may activate the PI3K pathway by 3 distinct mechanisms: direct interaction and phosphorylation of AKT (12, 13); interaction and activation of PI3K (14, 15); and reversal of PTEN activity (16).

Because local invasion is a critical determinant of both morbidity and mortality for HNSCC, systemic therapy that both decreases local invasion and induces significant cancer cell cytotoxicity would be ideal. Given that c-Src inhibition already results in a significant decrease in invasion, we sought in this study to understand the mechanisms underlying the effects of c-Src inhibition on cancer cell survival. We studied several signaling pathways known to interact with c-Src and discovered a correlation between the biological effects of c-Src inhibition and downstream signaling effects on the receptor tyrosine kinase c-Met. c-Met is known to signal both upstream and downstream from c-Src. It mediates resistance to epidermal growth factor receptor (EGFR) inhibition in lung cancer (17, 18) and c-Src inhibition in gastric cancer cell lines (19). Activation of c-Met by its ligand hepatocyte growth factor (HGF) is observed in HNSCC cell lines and tumors (20, 21); this activation stimulates migration and invasion and inhibits apoptosis of HNSCC cells (20, 22–25). We hypothesized that persistent c-Met activation following c-Src inhibition mediates resistance to apoptosis and cell cycle arrest.

Materials and Methods

Materials

Antibodies used in the Western blot analysis included c-Met (Santa Cruz Biotechnology); pSFK (Y416), pSTAT3 (Y705), pPDK1 (S241), pan-AKT, pAKT (S473), and pMet (Y1234/1235 and Y1349) (Cell Signaling Technology); HGF and pMet (Y1365) (Abcam), pMet (Y1003) (BD Bioscience), and β-actin (Sigma Chemical). For immunoprecipitation studies, agarose-conjugated c-Src antibody was obtained from Calbiochem and agarose-conjugated c-Met antibody from Santa Cruz Biotechnology. Dasatinib was purchased from The University of Texas MD Anderson Cancer Center pharmacy and prepared as a 10 mM stock solution in dimethyl sulfoxide (DMSO). PHA665752 and PF02341066 (crizotinib) were provided by Pfizer Pharmaceuticals and prepared as a 10 mM stock solution in DMSO. Human HGF Quantikine ELISA was purchased from R&D system.

Cell culture

Human HNSCC cell lines were obtained from Dr. Jeffrey Myers (MD Anderson Cancer Center, Houston, Texas) and maintained as described previously (10). Short tandem repeat profiling was performed on cellular DNA submitted to the Johns Hopkins University Fragment Analysis Core facility (Baltimore, MD). All cell lines were validated by cross-comparing their allelic short tandem repeat patterns, generated with the PowerPlex 1.2 platform (Promega), to the American Type Culture Collection repository database. Cells were passed in culture no more than 6 months after being thawed from authenticated stocks.

MTT assay

Cytotoxicity was assessed by the MTT assay as described elsewhere (9). For each experimental condition, at least 4 wells were treated. Cytotoxic effects and the combination index were calculated by using the Chou–Talalay equation, which takes into account both the potency (IC_{50}) and shape of the dose-effect curve (26–28), using CalcuSyn software (Biosoft).

Cell cycle and apoptosis assays

For the cell cycle analysis, cells were harvested, fixed, and stained with propidium iodide as previously described (29). DNA content was analyzed on a cytofluorimeter by fluorescence-activated cell sorting analysis (FACS, FACScan; Becton Dickinson) using ModFit software (Verity Software House). To analyze apoptosis, cells were fixed and subjected to terminal deoxynucleotidyl transferase biotin-dUTP nick-end labeling (TUNEL) staining according to the manufacturer's protocol (APO-BRDU kit; Phoenix Flow Systems Inc.) as described previously (29).

Transfection with small interfering RNA

Cells were harvested, washed, and suspended ($\times 10^6$ cells/100 mL) in Nucleofector-V solution (Amaxa), and

small interfering RNA (siRNA) (200 pmol/100 mL) was added. Cells were electroporated (U-31 Nucleofector program, Amaxa) and then immediately diluted with prewarmed 500 μL Dulbecco's modified essential medium and plated onto 6-well plates. The medium was changed after 16 hours. All c-Src and c-Met siRNAs were predesigned as sets of 4 independent sequences (siGENOME SMARTpool, Dharmacon Inc.). Controls included cells transfected with a nontargeting (scrambled) siRNA and mock transfected cells (i.e., no siRNA).

Immunoprecipitation and Western blot analysis

Western blot analysis and immunoprecipitation were performed as previously described (9, 29). Briefly, cells were subjected to lysis on ice and lysates centrifuged at 15,000 rpm for 5 minutes at 4°C. For the immunoprecipitation, equal amounts of the protein cell lysate supernatant (500 mg) were precleared with Protein A and G Sepharose beads (Invitrogen Corporation). The precleared lysate was incubated with 5 μg of either the agarose-conjugated c-Met or the c-Src primary antibody overnight. The immunoprecipitates containing agarose beads were washed 4 times with immunocomplex wash buffer [50 mmol/L Tris-HCl (pH 7.5), 100 mmol/L NaCl, 1% Triton X-100, 1 mmol/L EGTA, 1 mmol/L EDTA, 1% glycerol, 20 μg/mL leupeptin, 10 μg/mL aprotinin, 1 mmol/L phenylmethylsulfonyl fluoride, 1 mmol/L sodium vanadate] and boiled with 1× sample buffer for 5 minutes. For both the immunoprecipitation and the Western blot, equal protein aliquots were resolved by sodium dodecyl sulfate polyacrylamide gel electrophoresis (SDS-PAGE), transferred to nitrocellulose membranes, immunoblotted with primary antibody, and detected with horseradish peroxidase–conjugated secondary antibody (Bio-Rad Laboratories) and ECL reagent (Amersham Biosciences).

In vitro kinase assay

In vitro kinase assays were performed as previously described (29). Briefly, Tu167 and Osc-19 cells were incubated with 100 nM dasatinib, DMSO (vehicle control), or 2 μM PHA665752 for 7 hours before cells were subjected to lysis, and c-Met or c-Src was immunoprecipitated as described in the previous paragraph. The immunocomplexes were washed and resuspended in a kinase assay reaction buffer that contained 15 microCi [γ^{32}P]ATP. During the kinase assay, 100 nM dasatinib or 2 μM PHA665752 was added to their respective samples. The reaction was terminated after 30 minutes at room temperature with sample buffer, and boiled immunocomplexes were separated by 8% SDS-PAGE. Radiolabeled proteins were detected by autoradiography. When c-Src and c-Met were assayed together, both were independently immunoprecipitated and then the immunoprecipitated fractions were combined in the kinase assay.

Orthotopic nude mouse models

All animal procedures were done in accordance with the Institutional Animal Care and Use Committee's policies. Osc-19-LN5-Rluc cells were injected submucosally into the tongues of athymic nude mice as previously described (30). Mice that developed tumors were randomized into four treatment groups: vehicle alone (control), crizotinib [PF02341066 (20 mg/kg/d)] alone, dasatinib alone (20 mg/kg daily), or dasatinib plus crizotinib; all agents were administered by oral gavage. Tumor volume was estimated by direct measurement using calipers and *in vivo* bioluminescence imaging on days 1, 5, and 9 as described (30). Mice were sacrificed on day 10 and tumors were dissected. Mice were examined for regional and distant metastases. The tongue tumors were homogenized and subjected to Western blotting.

Results

Oral squamous carcinoma cell lines have diverse sensitivities to SFK inhibition

We used a panel of 11 independent, authenticated HNSCC cell lines derived from the oral cavity to measure the effects of SFK inhibition on cytotoxicity, proliferation, and survival. All cell lines were incubated with the SFK inhibitor dasatinib, and cytotoxicity was measured by the 3-(4,5-dimethylthiazol-2-yl)-2,5-diphenyltetrazolium bromide (MTT) assay. Median inhibitory concentrations (IC_{50}) for those cell lines ranged from 45 nM to >5 μM (Table 1). We also determined the effect of SFK inhibition on cell cycle progression and apoptosis in a panel of 7 lines with diverse sensitivities to dasatinib (Fig. 1). Dasatinib did not affect proliferation or survival in resistant cell lines (IC_{50} values >100 nM) but affected both qualities in 2 of 3 sensitive lines.

Prolonged exposure to SFK inhibition leads to acquired resistance

To study resistance to SFK inhibition in an isogenic setting, the sensitive cell line Tu167 was incubated with increasing concentrations of dasatinib. Ultimately, two cell lines (Tu167R1 and Tu167R2) were able to grow in 300 nM dasatinib with doubling times similar to that of the parent cell line. Both cell lines had a significantly higher IC_{50} value than Tul67 (Table 1) and did not undergo cell cycle arrest or apoptosis upon exposure to dasatinib (Fig. 1).

Inhibition of SFK results in c-Met inhibition in HNSCC cells that are sensitive to SFK inhibition

To determine the mechanisms underlying SFK resistance, we investigated signaling pathways that cooperate with or are downstream of SFK in epithelial malignancies. We observed that SFK inhibition led to inhibition of c-Met in sensitive cell lines (Fig. 2A–C) but not in resistant lines (Fig. 2A–D). Moreover, the PI3K pathway (AKT or PDK1) was inhibited in cell lines that underwent apoptosis (Tu167, PCI-13) when exposed to dasatinib (Fig. 2), whereas the effects on the mitogen-activated protein kinase pathway, as measured by pERK1/2, were variable (data not shown). Surprisingly, we also observed that c-Met and AKT were not inhibited even at elevated concentrations of dasatinib (200 nM) in Tu167R2, whereas dasatinib did

Table 1. IC_{50} values for dasatinib in HNSCC cell lines

Cell line	Source	IC_{50} (nM)	Interpretation
Tu167	Oral cavity, floor of mouth	45 ± 8	Sensitive
TR146	Oral cavity	67 ± 2	Sensitive
PCI-24	Oral cavity, tongue	53 ± 14	Sensitive
PCI-13	Oral cavity	96 ± 15	Sensitive
HN5	Oral cavity, tongue	140 ± 79	Intermediate
UMSCC47	Oral cavity, tongue	160 ± 34	Intermediate
UMSCC2	Oral cavity, alveolar ridge	180 ± 37	Intermediate
UMSCC15A	Oral cavity	186 ± 15	Intermediate
OSC19	Oral cavity	312 ± 36	Resistant
LN686	Oral cavity, tongue	324 ± 101	Resistant
Tu167R2	Oral cavity, floor of mouth	803 ± 189	Resistant
Tu167R1	Oral cavity, floor of mouth	>1000	Resistant
Tu138	Oral cavity	>5000	Resistant

inhibit SFKs in this isogenic resistant cell line (Fig. 2D). Dasatinib did not inhibit SFK in Tu167R1 even at elevated concentrations (200 nM), demonstrating that direct resistance of the target (i.e., SFK) to the drug is the mechanism for these cells' insensitivity to the cytotoxic effects of dasatinib (Supplementary Fig. 1). Thus, we did not further study c-Src and c-Met interactions in Tu167R1.

Specific inhibition of c-Src leads to c-Met inhibition in sensitive HNSCC cells

To determine whether the inhibition of c-Met was due to inhibition of SFKs or to an off-target effect of dasatinib, c-Src was specifically depleted by using small interfering RNA (siRNA). In sensitive cells, c-Src knockdown led to substantial inhibition of c-Met, whereas in resistant cells, c-Src depletion did not affect c-Met activation (Fig. 2E). Similar to the results with dasatinib, specific c-Src knockdown led to inhibition of AKT in sensitive cells and not in resistant cell lines.

Baseline expression or activation of c-Src or c-Met did not predict biological response to SFK inhibitors

We hypothesized that cell lines with high basal levels of activated c-Src or c-Met would be more likely to be sensitive to SFK inhibition. We examined the basal expression and activation of these proteins in 8 HNSCC lines (Supplementary Fig. 2) that had previously been characterized (Table 1) and found no such correlation.

c-Met is a c-Src substrate in both sensitive and resistant cell lines

To determine if c-Met is a direct c-Src substrate, we incubated isolated c-Met, c-Src, or both from resistant

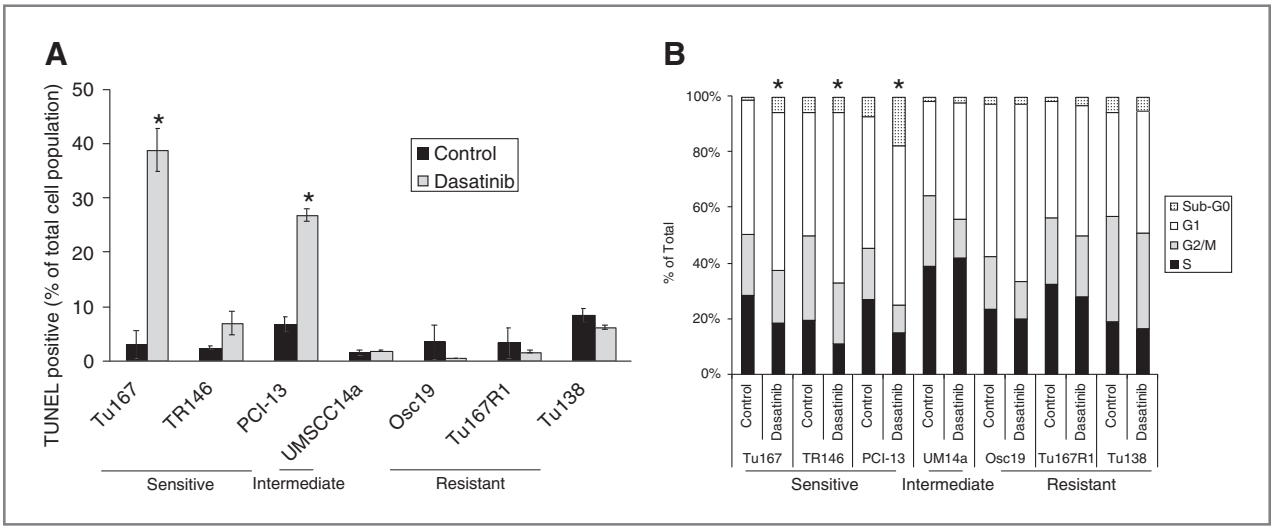

Figure 1. The effect of SFK inhibition on apoptosis and cell cycle in HNSCC cell lines. Cells were treated with vehicle control or 100 nM dasatinib for 24 hours and analyzed by TUNEL staining (A) or stained with propidium iodide and analyzed by FACS (B). The proportion of apoptotic cells or cells in each cell cycle phase is graphed as percentage of the total. Bars, *SD*. *$P \leq 0.05$ (B, for the effect on S-phase) versus vehicle control.

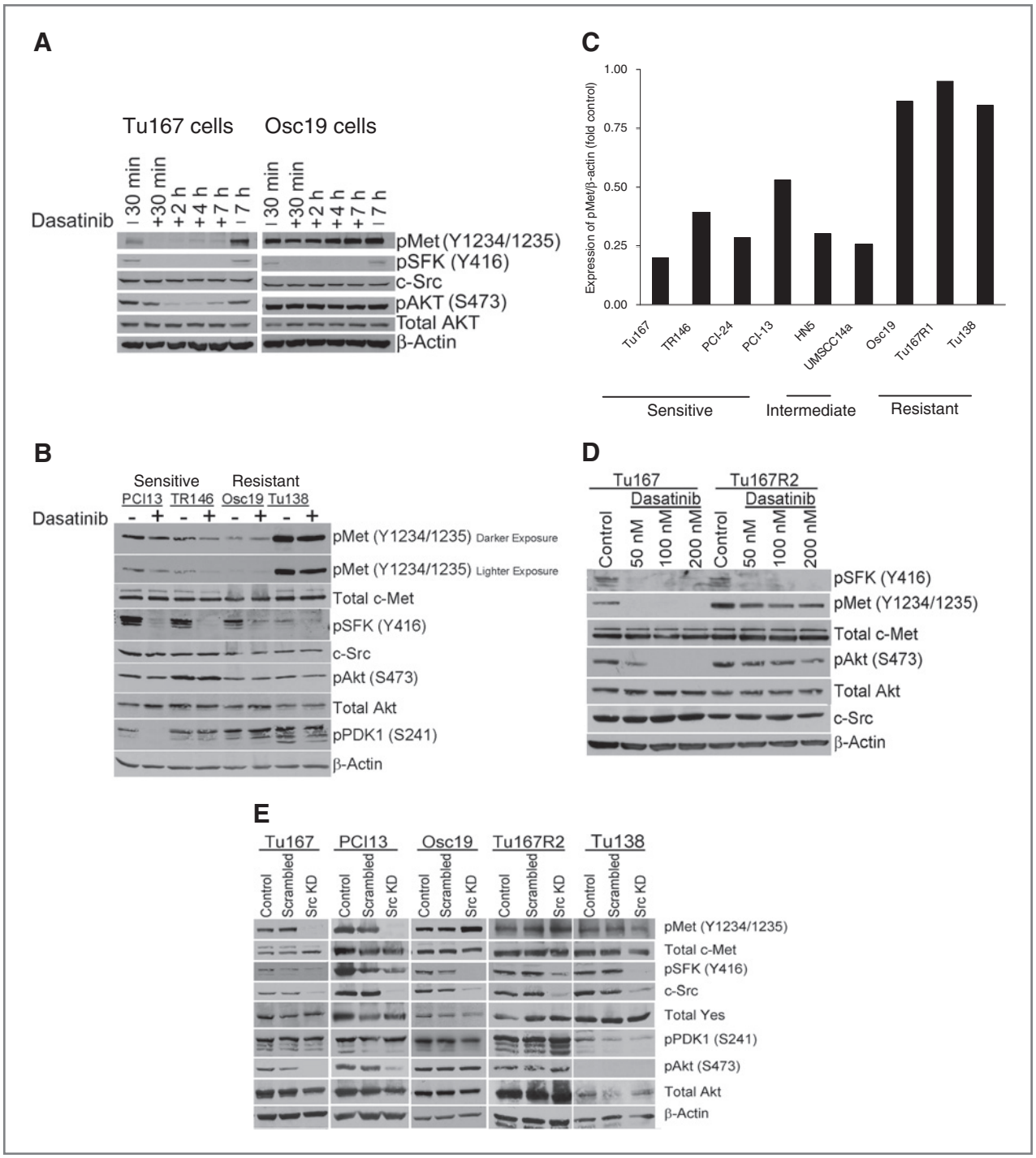

Figure 2. The effect of SFK inhibition or depletion on c-Met and AKT phosphorylation in a panel of sensitive and resistant HNSCC cell lines. Nine HNSCC cell lines were incubated with 100 nM dasatinib (A, B, C) for indicated times (A) or for 7 h (B, C, D) and analyzed by Western blotting. C, Western blots for activated Met (pMet Y1234/1235) from 9 HNSCC cell lines were analyzed by densitometry and normalized to beta-actin and control (i.e., vehicle treated). E, HNSCC cells were transfected with c-Src–specific siRNA or scrambled siRNA, or mock transfected, and the signaling molecules were analyzed by Western blotting 72 hours after transfection. KD, knockdown.

(Osc-19) and sensitive (Tu167) cell lines and measured kinase activity by an *in vitro* kinase assay. As expected, dasatinib and c-Met inhibitor PHA665752 inhibited c-Src and c-Met kinase activity respectively and specifically (Fig. 3A and B, lanes 1–6). In both cell lines, inhibition of c-Src led to decreased expression of phosphorylated c-Met

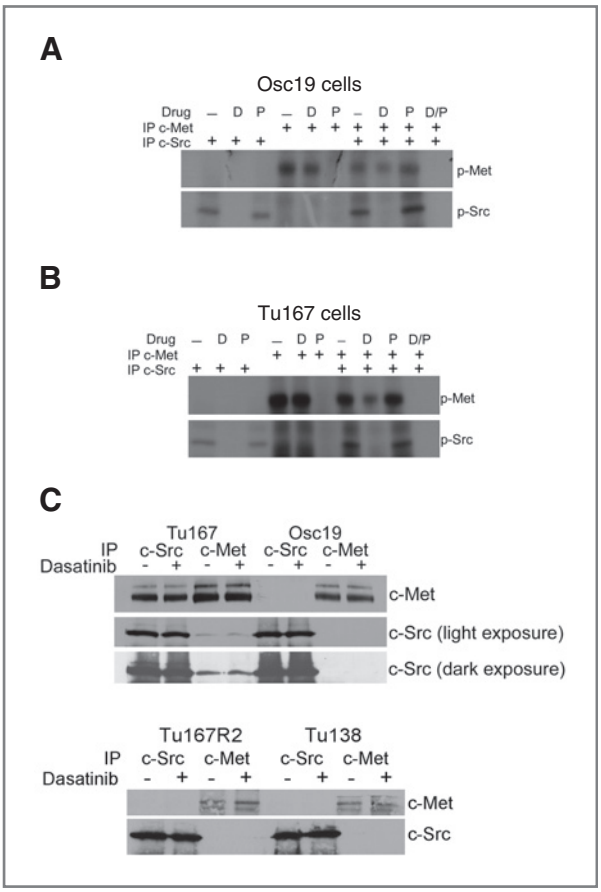

Figure 3. c-Met and c-Src interactions as isolated proteins and in intact cells. (A, B) c-Src or c-Met was immunoprecipitated (IP) from 2 HNSCC cell lines and incubated with 2.5 μM PHA665752 (P) or 100 nM dasatinib (D) or in combination (D/P) as indicated, and kinase activity was measured by the *in vitro* kinase assay. (C) c-Src and c-Met were immunoprecipitated from HNSCC cells that were incubated with 100 nM dasatinib or vehicle control for 7 h. Immunocomplexes were resolved by 11% SDS-PAGE and blotted with c-Src or c-Met antibodies.

(Fig. 3A and B, lanes 7 vs. 8), but the inhibition of c-Met did not affect expression of phosphorylated c-Src (Fig. 3A and B, lanes 7 vs. 9). Furthermore, in the presence of PHA665752 and c-Src, c-Met was phosphorylated, confirming that c-Met is a direct c-Src substrate (Fig. 3A and B, lane 9) and acts as a downstream signaling molecule for c-Src kinase.

c-Src and c-Met interactions are distinct in HNSCC cell lines

Although the *in vitro* kinase assay demonstrated that c-Met is a c-Src substrate in both sensitive and resistant cell lines, c-Src knockdown or inhibition reduced c-Met activation in some HNSCC cell lines but not others. These data suggest that there is no intrinsic change in the c-Src or c-Met molecules, but that the interaction between c-Src and c-Met differs in sensitive and resistant intact cells. To investigate this possibility, we immunoprecipitated c-Met or c-Src from sensitive and resistant cells (Fig. 3C). In Tu167 cells, an interaction between c-Src and c-Met was demonstrated by the immunoprecipitation of both c-Src and c-Met. No such interaction was demonstrated in resistant cells.

The effect of SFK inhibition on c-Met is not mediated via the release of ligand

We examined whether the release of HGF mediates SFK's effect on c-Met activation. In a panel of 6 HNSCC cell lines with diverse sensitivities to dasatinib (Tu167, Tu167R2, PCI13, Osc19, Tu138, and TR146), we did not detect HGF secretion by ELISA into the cell culture medium in control or dasatinib-treated cells (up to 48 hours incubation). Similarly, cellular levels of HGF did not change following dasatinib treatment in any of these cell lines (Fig. 4A). Exogenous HGF led to the activation of c-Met on 4 distinct sites (Fig. 4A). In sensitive cells, dasatinib inhibited the phosphorylation of Y1234/1235 (activation loop), Y1365 (morphology/motility), and Y1349 (Gab1 binding) in both the presence and absence of exogenous HGF but did not affect Y1003 (ubiquitination). All cell lines expressed the adaptor protein Gab1.

EGFR contributes to c-Met activation in resistant cell lines

Previous reports have demonstrated cross-talk between EGFR and c-Met. To determine if EGFR contributes to c-Met activation in HNSCC, cells were incubated with the EGFR inhibitor erlotinib, dasatinib, or a combination of both agents (Fig. 4B). In all cell lines tested, EGFR inhibition did lead to c-Met inactivation with no effect of SFK activation. The combination of erlotinib and dasatinib resulted in a cooperative effect on c-Met activation and a significant decrease in AKT activation in the resistant cell lines. Similarly, our previous work demonstrated that dasatinib and erlotinib are additive in HNSCC cells *in vitro* (9).

SFK and c-Met inhibitors show synergistic effect on HNSCC cell viability *in vitro* and *in vivo*

Given that c-Met is not inhibited in cell lines that are resistant to SFK inhibition, we hypothesized that persistent c-Met activation may mediate this resistance. To test this, a panel of 7 HNSCC cell lines with diverse sensitivities to SFK inhibition was incubated with dasatinib, PHA665752, or the combination, and cytotoxicity was measured by the MTT assay. We also calculated the combination index for the drug combination (Table 2). A combination index value of less than 1 indicates synergy; a value equal to 1 indicates an additive effect; and a value greater than 1 indicates antagonism. Representative cytotoxicity data are shown in Figure 5A and B.

None of the cell lines demonstrated the extreme sensitivity to PHA-665752 that occurs in cells with amplified c-Met (IC_{50} < 100 nM) (31). However, 3 of the 7 lines demonstrated IC_{50} values that were less than or close to 2.5 μM, a concentration at which we observed significant inhibition of c-Met (Supplementary Fig. 3); inhibition of c-Met was incomplete at a concentration of 1 μM

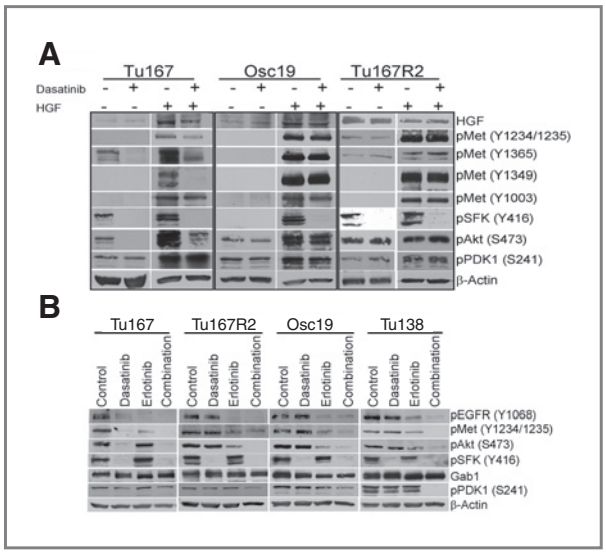

Figure 4. Effect of HGF and EGFR inhibition on c-Met activation. (A) HNSCC cells were serum starved and then incubated with 50 ng/ml HGF (5 min) and/or 100 nM dasatinib (7 h) as indicated and signaling molecules were analyzed by Western blotting. (B) HNSCC cells were incubated with 1 μM erlotinib, 100 nM dasatinib, vehicle control, or a combination of both drugs for 7h and then analyzed by Western blotting.

(unpublished data). As hypothesized, the combination of c-Met and SFK inhibition was synergistic in the dasatinib-resistant cell lines. Consistent with the cytotoxicity data, this finding shows that the combination resulted in significantly more apoptosis than either agent alone (Fig. 5C). Surprisingly, the combination was also synergistic in the dasatinib-sensitive (Tu167, TR146) and intermediate (UMSCC14a) cell lines, suggesting that inhibition of the residual c-Met activation following SFK inhibition was adequate to enhance cytotoxicity (Table 2).

As expected, PHA665752 inhibited c-Met and dasatinib inhibited c-Src in HNSCC cell lines (Fig. 5D). We also examined the effect of these inhibitors on activated ErbB3 because ErbB3 can mediate c-Met's effects in EGFR inhibitor-resistant non–small cell lung cancer (NSCLC) cell lines (17). However, we did not find any consistent effect of c-Met or SFK inhibition on activated ErbB3. In most of these cell lines, the combination led to decreased signaling through the PI3K pathway (PDK1 or AKT).

Consistent with our *in vitro* data, we also observed that the combination of c-Src and c-Met inhibition reduced tumor size *in vivo* (Fig. 5E and Supplementary Fig. 4). In the *in vivo* studies, we utilized crizotinib due to the poor oral bioavailability of PHA665752. The single agents alone did not significantly affect tumor size. Western blotting of tumors confirmed that the drugs affected their targets (Supplementary Fig. 5). There was a statistically nonsignificant trend toward decreased nodal metastasis in mouse treated with the combination (3 of 20 nodes examined contained tumor, 15%) compared to control (7/28, 25%) or single agents [dasatinib (8/27, 30%) or crizotinib (4/21, 19%)]. The number of mice with nodal metastasis ranged from 42% to 56%.

We previously observed that c-Src inhibition led to a universal inhibition of invasion and migration independent of its effects on apoptosis (10). Both PHA665752 and dasatinib inhibited invasion and migration; the combination was more effective than the single agents (Supplementary Fig. 6). The effect was independent of the effects of either drug on cytotoxicity.

Specific depletion of c-Src and c-Met in HNSCC cell lines

To determine if the enhanced cytotoxic effects of dasatinib and PHA665752 were due to specific effects of the drugs on c-Src and c-Met, respectively, we specifically knocked down c-Src and c-Met with siRNA and measured the surviving cells by using an MTT assay (Fig. 6 and Supplementary Fig. 7). In both Osc-19 and Tu167 cells, c-Src depletion alone led to a decrease of about 25% in cell number, and c-Met depletion alone led to a decrease of about 15% in cell number ($P < 0.05$ vs. control or scrambled siRNA). Consistent with the pharmacologic

Table 2. Median effects of dasatinib and PHA665752 as single agents and in combination

Cell line	Single agent, IC_{50}		Combination, IC_{50}		Combination index simulations $F_a = 0.5$	Interpretation
	Dasatinib (nM)	PHA665752 (μM)	Dasatinib (nM)	PHA665752 (μM)		
Tu167	45 ± 7.7	6.8 ± 2.1	20 ± 6.6	1.6 ± 0.53	0.68 ± 0.15	Synergistic
TR146	67 ± 2.3	2.6 ± 1.0	27 ± 13	0.53 ± 0.27	0.60 ± 0.22	Synergistic
UMSCC14a	186 ± 15	1.9 ± 0.7	28 ± 18	0.57 ± 0.37	0.44 ± 0.26	Synergistic
Osc19	312 ± 36	8.7 ± 4.9	107 ± 39	1.1 ± 0.39	0.47 ± 0.12	Synergistic
Tu167R2	803 ± 189	22 ± 1.4	268 ± 86	1.1 ± 0.34	0.38 ± 0.09	Synergistic
Tu167R1	>1000	6.5 ± 2.2	316 ± 129	1.3 ± 0.50	0.41 ± 0.13	Synergistic
Tu138	>5000	2.1 ± 0.3	148 ± 19	1.5 ± 0.02	0.72 ± 0.07	Synergistic

NOTE: Data presented as mean ± SD.

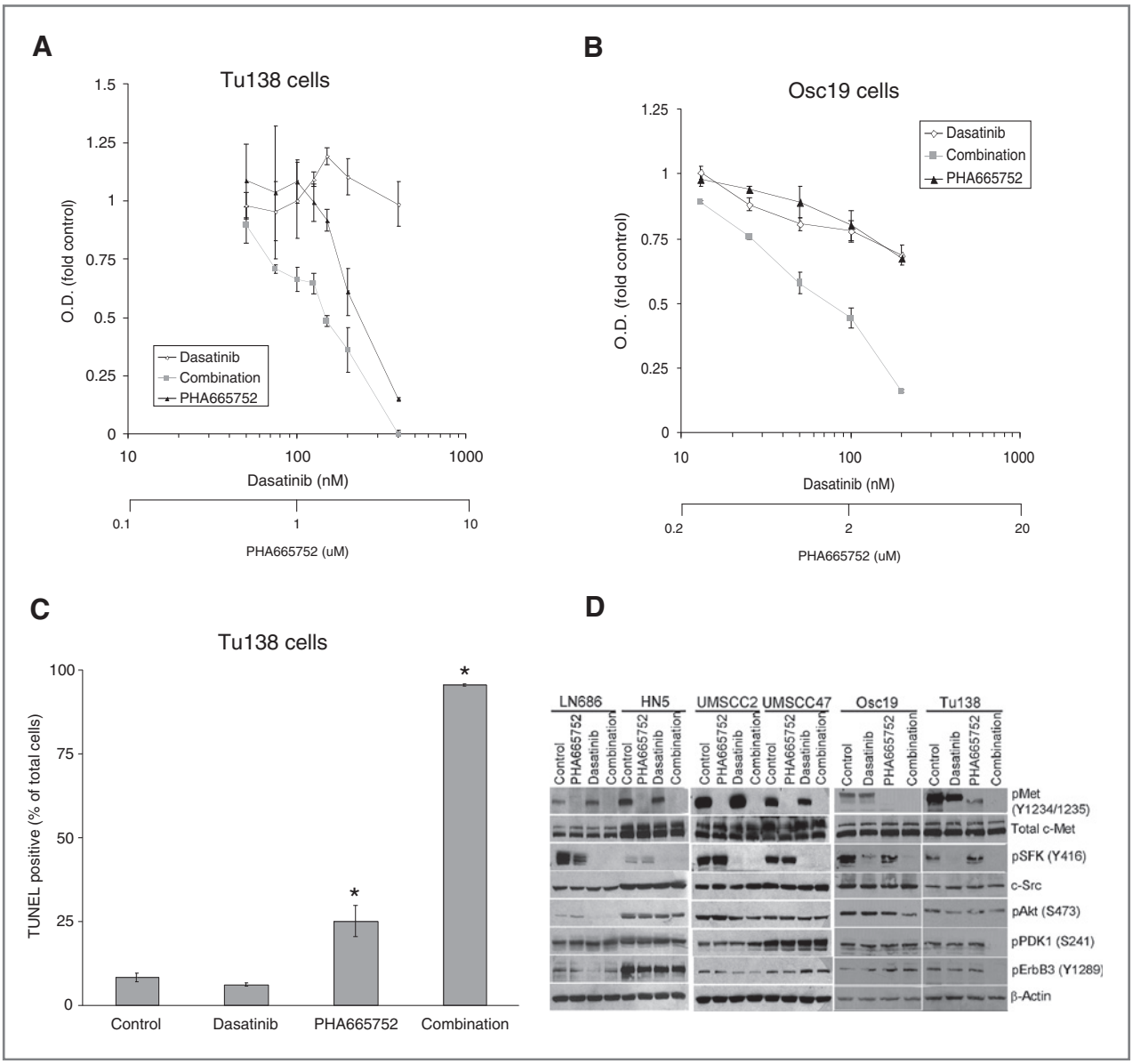

Figure 5. The combination of SFK and c-Met inhibition resulted in synergistic cytotoxic and signaling effects *in vitro* and *in vivo*. Tu138 (A) and Osc19 (B) cells were treated with PHA665752 alone, dasatinib alone, or the 2 agents combined in a fixed ratio at the indicated doses for 72 h. The number of viable cells was determined by MTT assay (O.D., optical density) and expressed as fold control (vehicle alone). C, Tu138 cells were treated with 100 nM dasatinib, 2 μM PHA665752, or the combination for 24 h and analyzed by TUNEL staining using FACS analysis. D, HNSCC cells were treated with 100 nM dasatinib, 2.5 μM PHA665752, or both for 7 h and analyzed by Western blotting with the indicated antibodies.

data (Table 2), the results show that the combination was more effective than either of the single siRNAs, with reductions in cell number of 36% for Tu167 and 54% for Osc-19 ($P < 0.05$ vs. control or scrambled or c-Src alone or c-Met alone). As we previously observed (29), the effect of c-Src knockdown was markedly less cytotoxic than SFK inhibition with dasatinib, probably because of 3 factors: dasatinib inhibits all SFKs (not just c-Src), dasatinib is a much more effective c-Src inhibitor than siRNA, and dasatinib likely has off-target effects that contribute to its cytotoxicity (32).

Discussion

In this study we sought to identify pathways leading to cytotoxicity downstream of c-Src inhibition and demonstrated that sustained c-Met activation mediates cell survival following c-Src inhibition. We observed a correlation

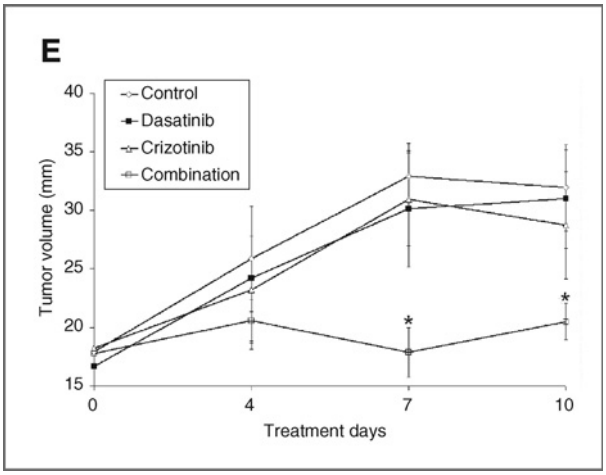

Figure 5. (Cont'd) (E) Mice bearing orthotopic tongue tumors (Osc19 cells transfected with luciferase) were treated with crizotinib alone, dasatinib alone, or the 2 agents combined and tumor size was measured. *P* values for the combination at 7 days were 0.002 (vs. control), 0.03 (vs. dasatinib), and 0.01 (vs. crizotinib). *P* values for the combination at 10 days were 0.007 (vs. control), 0.02 (vs. dasatinib), and 0.05 (vs. crizotinib). (*$P \leq 0.05$ versus vehicle control).

between the effects of c-Src inhibition on c-Met activity and its effects on apoptosis. Although c-Met and c-Src isolated from sensitive cells and from resistant cells behave similarly, the interaction between c-Met and c-Src in intact sensitive and resistant cell lines differs. This implies that there are factors promoting c-Src/c-Met interaction in sensitive cells and/or factors inhibiting such interaction in resistant cells; this will be tested in our future studies. We speculate that these factors are adaptor proteins that can affect c-Src or c-Met localization and/or protein–protein binding and interaction. We investigated the biological

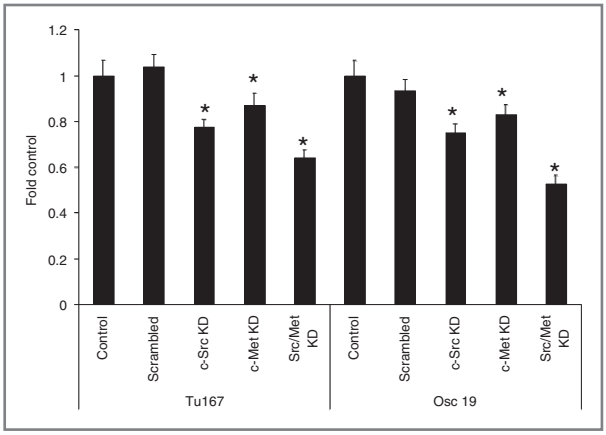

Figure 6. Depletion of c-Met enhances the cytotoxicity of c-Src depletion. Tu167 and Osc19 cells were transfected with c-Src–specific siRNA (KD, knockdown), c-Met specific siRNA, both, or nonspecific (scrambled) controls. The number of viable cells was estimated 96 h after transfection by an MTT assay and expressed as fold control (mock transfected). Bars, SD. *$P \leq 0.05$ versus vehicle control.

consequences of this interaction and discovered that SFK inhibitor dasatinib and c-Met inhibitor PHA-665752 have synergistic cytotoxic and proapoptotic effects and that the combination of c-Src and c-Met siRNA has enhanced cytotoxicity. c-Met inhibition alone (by siRNA or PHA665752) had a statistically significant but minimal effect on cytotoxicity, demonstrating that c-Src mediates some of its effects independently of c-Met. Together these data support a model in which c-Src and c-Met cooperate to maintain cell survival in sensitive HNSCC cells. In resistant cell lines, alternative pathways must exist that allow cell survival despite complete c-Src and c-Met inhibition (Supplementary Fig. 8).

We did not expect there to be only a single mechanism of resistance to c-Src inhibition. This situation is analogous to resistance of cancers to targeted agents and to cytotoxic chemotherapy drugs, which is mediated by diverse mechanisms (33). For example, resistance to EGFR inhibitors in lung cancer can be mediated by additional mutations in EGFR (T790M), amplification of c-Met (17), activation of the insulin growth factor receptor (34), and other undefined mechanisms. Correspondingly, an unbiased approach to identifying proteins with significant changes in tyrosine phosphorylation upon c-Src activation identified 136 proteins with increased tyrosine phosphorylation, including c-Met (35). These data are supported by the finding that gastric cell lines that express c-Met are resistant to SFK inhibition–induced apoptosis (19). We also demonstrated that the reactivation of STAT3 following sustained c-Src inhibition may contribute to resistance to c-Src inhibition (29). Even though alternative mechanisms may exist, however, the combination of c-Met and c-Src inhibitors was synergistic in all cell lines tested, suggesting that this is a rational combination for future clinical studies.

Cross-talk between c-Met and c-Src has been demonstrated in other epithelial tumors and often involves Her family members. Serum starvation of bladder cancer cell lines leads to release of growth factors that activate EGFR, which subsequently activates c-Met in a c-Src–dependent manner. This process is not dependent upon ligand-mediated activation of c-Met, rather the c-Met is activated by c-Src (36). Similarly, c-Met can be activated by EGFR in human hepatoma cell lines (37), anaplastic thyroid cancer cells (38), and lung cancer (39), but the role of c-Src in these systems was not investigated. In a separate study, pharmacologic inhibition of SFKs led to decreased levels of phosphorylated c-Met in 4 of 5 colon cancer cell lines, but the mechanism was not defined (40).

Signaling between c-Src and c-Met can be bidirectional. Activation of c-Met by HGF in breast cancer cell lines leads to the interaction of c-Src and c-Met and subsequent activation of c-Src. The kinase activity of c-Src is required for HGF-induced cell motility and anchorage-independent growth (41). In our study, however, the inhibition of c-Met did not affect c-Src activation in intact cells and HGF was not affected by dasatinib. Similarly, c-Src was not a direct c-Met substrate. These differences may be due to the dif-

ference in cell type (HNSCC vs. breast) or the different approaches employed to manipulate c-Met activation (i.e., ligand stimulation vs. kinase inhibition). Moreover, c-Met inhibition alone leads to cytotoxicity and AKT inhibition in some cancer cell lines (42) and in HNSCC *in vivo* (21), but in our HNSCC *in vitro*, this was not observed.

In lung cancer cell lines, c-Met can mediate resistance to EGFR inhibition. When NSCLC cell lines with activating EGFR mutations were incubated with increasing concentrations of the EGFR inhibitor gefitinib, the resulting gefitinib-resistant NSCLC cells had amplified c-Met and persistent activation of ErbB3 and AKT following exposure to gefitinib. Although these cells were resistant to both gefitinib and PHA665752, the combination resulted in growth inhibition and suppression of AKT and ErbB3 phosphorylation. We also observed suppression of ErbB3 phosphorylation with the combination of dasatinib and PHA665752, but in only 1 of 6 cell lines tested (Tu138). c-Src inhibition had no observed effect on activated EGFR in HNSCC cells (9). EGFR inhibition did lead to c-Met inhibition in resistant cell lines. In NSCLC cell lines, activation of ErbB3 by c-Met was not c-Src dependent (17). Similarly, in breast cancer cell lines, c-Met activation can mediate EGFR resistance, but through a mechanism that is distinct from that of NSCLC. In breast cancer cells, c-Met activation leads to EGFR kinase-independent phosphorylation of EGFR via a c-Src–dependent mechanism. Thus, despite the presence of an EGFR kinase inhibitor, EGFR can still be phosphorylated and contribute to cell growth (43). Interestingly, engagement of EGFR signaling can mediate resistance of NSCLC cells to c-Met inhibition *in vitro*, further demonstrating an intimate link between these two pathways in lung cancer (44).

Any study using pharmacological agents is limited by drug specificity. Although PHA-665752 did drastically reduce the IC_{50} for dasatinib, it brought this value into a range that we consider SFK specific (<100 nM) in only 2 of the 5 dasatinib-resistant cell lines (Osc-19 and UMSCC14a), suggesting that resistance in these lines may be "driven" by other signaling pathways that may include the JAK-STAT signaling axis (29). However, the enhanced cytotoxicity observed with the combination of c-Src and c-Met siRNA does demonstrate that these 2 specific pathways can cooperate to contribute to cell survival. At the concentrations we used, PHA665752 inhibits c-Met, Ron, Flk-1, and c-Abl (42) and dasatinib inhibits c-Abl, PDGFR, Btk, EphA2, and others (32, 45, 46).

In conclusion, this study offers new insights into the interaction of c-Src and c-Met in HNSCC cells. In cells that were sensitive to SFK inhibition, c-Met was a c-Src substrate and the 2 proteins interacted. This interaction did not occur in resistant cell lines even though the isolated c-Met was a c-Src substrate. This is the first study to demonstrate a potential mechanism by which c-Met activation can mediate resistance to SFK inhibition in only a subpopulation of cancer cells. The synergistic effects of SFK and c-Met inhibition may have important clinical implications for the treatment of HNSCC.

Disclosure of Potential Conflicts of Interest

F. Johnson, commercial research grant, advisory board, Bristol Myers Squibb.

Grant Support

This work was supported by the Head and Neck SPORE (P50 CA097007) and the generous donations of cancer patients and their families. FACS was funded by National Cancer Institute grant CA 16672.

The costs of publication of this article were defrayed in part by the payment of page charges. This article must therefore be hereby marked *advertisement* in accordance with 18 U.S.C. Section 1734 solely to indicate this fact.

Received June 18, 2010; revised November 3, 2010; accepted November 5, 2010; published OnlineFirst November 24, 2010.

References

1. Jemal A, Siegel R, Ward E, Hao Y, Xu J, Thun MJ. Cancer statistics. CA Cancer J Clin 2009;59:225–49.
2. Johnson FM, Gallick GE. SRC family nonreceptor tyrosine kinases as molecular targets for cancer therapy. Anticancer Agents Med Chem 2007;7:651–9.
3. Kim LC, Song L, Haura EB. Src kinases as therapeutic targets for cancer. Nat Rev Clin Oncol 2009;6:587–95.
4. Nam S, Kim D, Cheng JQ, Zhang S, Lee JH, Buettner R, et al. Action of the Src family kinase inhibitor, dasatinib (BMS-354825), on human prostate cancer cells. Cancer Res 2005;65:9185–9.
5. Rodier JM, Valles AM, Denoyelle M, Thiery JP, Boyer B. pp60c-src is a positive regulator of growth factor-induced cell scattering in a rat bladder carcinoma cell line. J Cell Biol 1995;131:761–73.
6. Hiscox S, Morgan L, Green TP, Barrow D, Gee J, Nicholson RI. Elevated Src activity promotes cellular invasion and motility in tamoxifen resistant breast cancer cells. Breast Cancer Res Treat 2006;97 (3):263–74.
7. Serrels A, Macpherson IR, Evans TR, Lee FY, Clark EA, Sansom OJ, et al. Identification of potential biomarkers for measuring inhibition of Src kinase activity in colon cancer cells following treatment with dasatinib. Mol Cancer Ther 2006;5:3014–22.
8. Summy JM, Trevino JG, Lesslie DP, Baker CH, Shakespeare WC, Wang Y, et al. AP23846, a novel and highly potent Src family kinase inhibitor, reduces vascular endothelial growth factor and interleukin-8 expression in human solid tumor cell lines and abrogates downstream angiogenic processes. Mol Cancer Ther 2005; 4: 1900–11.
9. Johnson FM, Saigal B, Tran H, Donato NJ. Abrogation of signal transducer and activator of transcription 3 reactivation after Src kinase inhibition results in synergistic antitumor effects. Clin Cancer Res 2007;13:4233–44.
10. Johnson FM, Saigal B, Talpaz M, Donato NJ. Dasatinib (BMS-354825) tyrosine kinase inhibitor suppresses invasion and induces cell cycle arrest and apoptosis of head and neck squamous cell carcinoma and non-small cell lung cancer cells. Clin Cancer Res 2005;11:6924–32.
11. Frame MC. Newest findings on the oldest oncogene; how activated src does it. J Cell Sci 2004;117:989–98.
12. Jiang T, Qiu Y. Interaction between Src and a C-terminal proline-rich motif of Akt is required for Akt activation. J Biol Chem 2003; 278: 15789–93.
13. Lodeiro M, Theodoropoulou M, Pardo M, Casanueva FF, Camina JP. c-Src regulates Akt signaling in response to ghrelin via beta-arrestin

signaling-independent and -dependent mechanisms. PLoS One 2009;4:e4686.
14. Gentili C, Morelli S, Russo De Boland A. Involvement of PI3-kinase and its association with c-Src in PTH-stimulated rat enterocytes. J Cell Biochem 2002;86:773–83.
15. Arcaro A, Aubert M, Espinosa del Hierro ME, Khanzada UK, Angelidou S, Tetley TD, et al. Critical role for lipid raft-associated Src kinases in activation of PI3K-Akt signalling. Cell Signal 2007;19:1081–92.
16. Lu Y, Yu Q, Liu JH, Zhang J, Wang H, Koul D, et al. Src family protein-tyrosine kinases alter the function of PTEN to regulate phosphatidylinositol 3-kinase/AKT cascades. J Biol Chem 2003;278:40057–66.
17. Engelman JA, Zejnullahu K, Mitsudomi T, Song Y, Hyland C, Park JO, et al. MET amplification leads to gefitinib resistance in lung cancer by activating ERBB3 signaling. Science 2007;316:1039–43.
18. Yoshida T, Okamoto I, Okamoto W, Hatashita E, Yamada Y, Kuwata K, et al. Effects of Src inhibitors on cell growth and epidermal growth factor receptor and MET signaling in gefitinib-resistant non-small cell lung cancer cells with acquired MET amplification. Cancer Sci 2010;101:167–72.
19. Okamoto W, Okamoto I, Yoshida T, Okamoto K, Takezawa K, Hatashita E, et al. Identification of c-Src as a potential therapeutic target for gastric cancer and of MET activation as a cause of resistance to c-Src inhibition. Mol Cancer Ther 2010; 9:1188–97.
20. Uchida D, Kawamata H, Omotehara F, Nakashiro K, Kimura-Yanagawa T, Hino S, et al. Role of HGF/c-met system in invasion and metastasis of oral squamous cell carcinoma cells in vitro and its clinical significance. Int J Cancer 2001;93:489–96.
21. Knowles LM, Stabile LP, Egloff AM, Rothstein ME, Thomas SM, Gubish CT, et al. HGF and c-Met participate in paracrine tumorigenic pathways in head and neck squamous cell cancer. Clin Cancer Res 2009;15:3740–50.
22. Matsumoto K, Nakamura T, Kramer RH. Hepatocyte growth factor/scatter factor induces tyrosine phosphorylation of focal adhesion kinase (p125FAK) and promotes migration and invasion by oral squamous cell carcinoma cells. J Biol Chem 1994;269:31807–13.
23. Dong G, Chen Z, Li ZY, Yeh NT, Bancroft CC, Van Waes C. Hepatocyte growth factor/scatter factor-induced activation of MEK and PI3K signal pathways contributes to expression of proangiogenic cytokines interleukin-8 and vascular endothelial growth factor in head and neck squamous cell carcinoma. Cancer Res 2001;61:5911–8.
24. Zeng Q, Chen S, You Z, Yang F, Carey TE, Saims D, et al. Hepatocyte growth factor inhibits anoikis in head and neck squamous cell carcinoma cells by activation of ERK and Akt signaling independent of NFkappa B. J Biol Chem 2002; 277:25203–8.
25. Bennett JH, Morgan MJ, Whawell SA, Atkin P, Roblin P, Furness J, et al. Metalloproteinase expression in normal and malignant oral keratinocytes: stimulation of MMP-2 and -9 by scatter factor. Eur J Oral Sci 2000;108:281–91.
26. Chou TC, Talalay P. Quantitative analysis of dose-effect relationships: the combined effects of multiple drugs or enzyme inhibitors. Adv Enzyme Regul 1984;22:27–55.
27. Chou TC. The Median-Effect Principle and the Combination Index for Quantitation of Synergism and Antagonism. San Diego, CA: Academic Press; 1991.
28. Chou TC, Riedeout D, Chou J, Bertino JR, Dulbecco R. Chemotherapeutic Synergism, Potential and Antagonism. San Diego, CA: Academic Press; 1991.
29. Sen B, Saigal B, Parikh N, Gallick G, Johnson FM. Sustained Src inhibition results in signal transducer and activator of transcription 3 (STAT3) activation and cancer cell survival via altered Janus-activated kinase-STAT3 binding. Cancer Res 2009;69:1958–65.
30. Sano D, Choi S, Milas ZL, Zhou G, Galer CE, Su YW, et al. The effect of combination anti-endothelial growth factor receptor and anti-vascular endothelial growth factor receptor 2 targeted therapy on lymph node metastasis: a study in an orthotopic nude mouse model of squamous cell carcinoma of the oral tongue. Arch Otolaryngol Head Neck Surg 2009;135:411–20.
31. Smolen GA, Sordella R, Muir B, Mohapatra G, Barmettler A, Archibald H, et al. Amplification of MET may identify a subset of cancers with extreme sensitivity to the selective tyrosine kinase inhibitor PHA-665752. Proc Natl Acad Sci USA 2006;103:2316–21.
32. Li J, Rix U, Fang B, Bai Y, Edwards A, Colinge J, et al. A chemical and phosphoproteomic characterization of dasatinib action in lung cancer. Nat Chem Biol 2010; 6:291–9.
33. Moscow J, Morrow CS, Cowan CH. Drug resistance and its clinical circumvention. In:Holland J, Frei EF, editors. Cancer Medicine. Sixth ed. Hamilton, Ontario: B.C. Decker; 2003.
34. Guix M, Faber AC, Wang SE, Olivares MG, Song Y, Qu S, et al. Acquired resistance to EGFR tyrosine kinase inhibitors in cancer cells is mediated by loss of IGF-binding proteins. J Clin Invest 2008;118:2609–19.
35. Leroy C, Fialin C, Sirvent A, Simon V, Urbach S, Poncet J, et al. Quantitative phosphoproteomics reveals a cluster of tyrosine kinases that mediates SRC invasive activity in advanced colon carcinoma cells. Cancer Res 2009;69:2279–86.
36. Yamamoto N, Mammadova G, Song RX, Fukami Y, Sato K. Tyrosine phosphorylation of p145met mediated by EGFR and Src is required for serum-independent survival of human bladder carcinoma cells. J Cell Sci 2006;119:4623–33.
37. Jo M, Stolz DB, Esplen JE, Dorko K, Michalopoulos GK, Strom SC. Cross-talk between epidermal growth factor receptor and c-Met signal pathways in transformed cells. J Biol Chem 2000;275: 8806–11.
38. Bergstrom JD, Westermark B, Heldin NE. Epidermal growth factor receptor signaling activates met in human anaplastic thyroid carcinoma cells. Exp Cell Res 2000;259:293–9.
39. Xu L, Nilsson MB, Saintigny P, Cascone T, Herynk MH, Du Z, et al. Epidermal growth factor receptor regulates MET levels and invasiveness through hypoxia-inducible factor-1alpha in non-small cell lung cancer cells. Oncogene 2010; 29:2616–27.
40. Emaduddin M, Bicknell DC, Bodmer WF, Feller SM. Cell growth, global phosphotyrosine elevation, and c-Met phosphorylation through Src family kinases in colorectal cancer cells. Proc Natl Acad Sci USA 2008;105:2358–62.
41. Rahimi N, Hung W, Tremblay E, Saulnier R, Elliott B. c-Src kinase activity is required for hepatocyte growth factor-induced motility and anchorage-independent growth of mammary carcinoma cells. J Biol Chem 1998;273:33714–21.
42. Christensen JG, Schreck R, Burrows J, Kuruganti P, Chan E, Le P, et al. A selective small molecule inhibitor of c-Met kinase inhibits c-Met-dependent phenotypes in vitro and exhibits cytoreductive antitumor activity in vivo. Cancer Res 2003;63:7345–55.
43. Mueller KL, Hunter LA, Ethier SP, Boerner JL. Met and c-Src cooperate to compensate for loss of epidermal growth factor receptor kinase activity in breast cancer cells. Cancer Res 2008; 68:3314–22.
44. McDermott U, Pusapati RV, Christensen JG, Gray NS, Settleman J. Acquired resistance of non-small cell lung cancer cells to MET kinase inhibition is mediated by a switch to epidermal growth factor receptor dependency. Cancer Res 2010;70:1625–34.
45. Bantscheff M, Eberhard D, Abraham Y, Bastuck S, Boesche M, Hobson S, et al. Quantitative chemical proteomics reveals mechanisms of action of clinical ABL kinase inhibitors. Nat Biotechnol 2007;25:1035–44.
46. Rix U, Hantschel O, Durnberger G, Remsing Rix LL, Planyavsky M, Fernbach NV, et al. Chemical proteomic profiles of the BCR-ABL inhibitors imatinib, nilotinib, and dasatinib reveal novel kinase and nonkinase targets. Blood 2007;110:4055–63.
47. Brannan JM, Sen B, Saigal B, Prudkin L, Behrens C, Solis L, et al. EphA2 in the early pathogenesis and progression of non-small cell lung cancer. Cancer Prev Res (Phila Pa) 2009;2:1039–49.